• Clinical Research •

3D choroidal vascularity index in hyperopic amblyopic eyes of preschool children: a case-control study using SS-OCTA

Yao-Ling Li, Ning Hua, Xiao-Yu Zeng, An-Qi Wang, Hui-Yu Wang, Xue-Han Qian

Tianjin Key Laboratory of Retinal Functions and Diseases, Tianjin Branch of National Clinical Research Center for Ocular Disease, Eye Institute and School of Optometry, Tianjin Medical University Eye Hospital, Tianjin 300384, China

Correspondence to: Xue-Han Qian. Department of Strabismus and Pediatric Ophthalmology, Tianjin Medical University Eye Hospital, Tianjin 300384, China. Xqian09@tmu.edu.cn

Received: 2025-06-29 Accepted: 2025-09-16

Abstract

● **AIM:** To evaluate the three-dimensional choroidal vascularity index (3D-CVI) in amblyopic eyes of preschool children compared with age-matched healthy controls using swept-source optical coherence tomography angiography (SS-OCTA).

● **METHODS:** A cross-sectional case-control study was conducted. Children aged between 4y and less than 7y diagnosed with hyperopic amblyopia were consecutively recruited between January 1, 2021 and May 30, 2024. Age-matched controls were selected from healthy children without ocular or systemic diseases. All participants underwent SS-OCTA scanning, and choroidal parameters—including 3D-CVI, choroidal vessel volume (CVV), and choroidal thickness (CT)—were analyzed in both foveal and parafoveal regions. Comparative and correlational analyses were conducted to examine differences between groups and to explore the relationship between best-corrected visual acuity (BCVA) and 3D-CVI.

● **RESULTS:** A total of 80 eyes (40 amblyopic and 40 age-matched controls) were included. 3D-CVI was significantly lower in the amblyopic group compared to controls in both the foveal [0.318 (0.2885-0.3525) *vs* 0.381 (0.3460-0.4212), $P<0.05$] and parafoveal [0.331 (0.2982-0.3589) *vs* 0.386 (0.3538-0.4293), $P<0.05$] regions. Similarly, CT was significantly higher in the amblyopic group than in the control group in both the foveal (438±67.3 *vs* 369±74.1 μm, $P<0.001$) and parafoveal regions (419±59.0 *vs* 353±67.5 μm, $P<0.001$), whereas CVV did not differ significantly between the two groups in either region ($P>0.05$). Furthermore, multivariate regression analysis showed that BCVA was positively associated with foveal 3D-CVI ($P=0.024$), whereas no such association was found in the parafoveal region.

● **CONCLUSION:** Hyperopic amblyopic eyes in preschool children show significantly lower foveal and parafoveal 3D-CVI compared to normal controls, suggesting a potential reduction in 3D-CVI during early refractive development. Lower foveal 3D-CVI is also associated with poorer BCVA, suggesting that 3D-CVI may serve as a valuable parameter for monitoring structural changes in hyperopic amblyopia.

● **KEYWORDS:** choroidal vascularity index; amblyopia; optical coherence tomography angiography; choroid; children

DOI:10.18240/ijo.2026.04.15

Citation: Li YL, Hua N, Zeng XY, Wang AQ, Wang HY, Qian XH. 3D choroidal vascularity index in hyperopic amblyopic eyes of preschool children: a case-control study using SS-OCTA. *Int J Ophthalmol* 2026;19(4):757-763

INTRODUCTION

Amblyopia ranks as the second most prevalent cause of visual impairment among children globally, with a prevalence ranging from 0.7% to 5.5% and varying based on factors like age, race, and ethnicity of the population under study. Failure to adequately address amblyopia during the critical period of visual development can result in enduring and potentially severe visual deficiencies throughout an individual's life[1]. Amblyopia is characterized as a developmental disorder of the central nervous system, marked by functional and morphological impairments in the visual cortex and lateral geniculate nucleus[2-3]. Recent research indicates that amblyopia may not only involve central nervous system irregularities but also potential structural changes within the eye, such as the retina, choroid, and ocular vasculature[4-7].

Although earlier optical coherence tomography studies on amblyopia predominantly focused on subfoveal choroidal thickness (CT), with the majority reporting increased thickness

in amblyopic eyes[7-9] despite some inconsistencies[10], advancements in swept-source optical coherence tomography angiography (SS-OCTA) technology—particularly its enhanced imaging depth—have extended the research focus to encompass potential changes in the choroidal vasculature.

Based on SS-OCTA imaging, the choroidal vascularity index (CVI) is a novel parameter that quantifies the proportion of the vascular area in relation to the total choroidal area. However, studies on CVI in amblyopic eyes have shown variability, possibly due to differences in study design, segmentation methods, and patient populations. Traditionally, CVI has been calculated from a single B-scan image at the foveal region, providing a two-dimensional assessment of the choroidal vasculature. Recent methods in image processing have introduced three-dimensional reconstruction techniques, allowing for a more comprehensive evaluation of the entire choroid. The three-dimensional CVI (3D-CVI) represents the ratio of choroidal vascular volume to total choroidal volume, offering a volumetric representation of vascularity, particularly in Sattler's layers. In comparison to two-dimensional CVI, 3D-CVI permits a more robust and representative analysis of choroidal vascular characteristics over a larger spatial area. Research on 3D-CVI in amblyopia is limited, with only one previous report known to us. In this study, we assessed the macular 3D-CVI in hyperopic amblyopic eyes of preschool children and compared it with age-matched controls.

PARTICIPANTS AND METHODS

Ethical Approval This case-control observational study was conducted in accordance with the tenets of the Declaration of Helsinki and was approved by the Ethics Committee of the Tianjin Medical University Eye Hospital (approval number: 2020KY-26). It was prospectively registered in the Chinese Clinical Trial Registry (ChiCTR), part of the WHO International Clinical Trials Registry Platform (ICTRP), under registration number ChiCTR2300072547. All participants were recruited from the outpatient department of the Tianjin Medical University Eye Hospital between January 1, 2021 and May 30, 2024. Informed consent was obtained from the parents or legal guardians of all participants after the nature and purpose of the study were explained.

Inclusion criteria for the amblyopic group included: 1) age between 4y and less than 7y; 2) newly diagnosed hyperopic amblyopia, including both anisometropic and isoametropic cases, with or without associated esotropia, meeting the criteria for unilateral amblyopia [interocular best corrected visual acuity (BCVA) difference ≥2 lines with normal fellow eye] or bilateral amblyopia (BCVA<20/40 in both eyes for ages 4 to <5y or <20/30 for ages≥5y). Exclusion criteria for the amblyopic group included: 1) history of other ocular abnormalities or systemic diseases; 2) prior optical correction or amblyopia treatment before enrollment; 3) poor cooperation during imaging or examination.

Inclusion criteria for the normal control group included: 1) age-matched to each case of the amblyopic group (aged 4 to <7y); 2) refractive error within the range of +3.00 to -3.00 diopters; 3) BCVA better than 20/20. Exclusion criteria for the normal control group included: 1) history of other ocular abnormalities or systemic diseases affecting vision; 2) inability to cooperate with optical coherence tomography angiography (OCTA) examination.

Prior to inclusion, all participants underwent a comprehensive medical history review and a detailed examination of both the anterior and posterior segments of the eye. Refractive status was assessed using cycloplegic retinoscopy. For cycloplegia, different protocols were applied to the amblyopic and control groups. In the amblyopic group, 1% atropine sulfate gel (SINQI Pharmaceutical Co., Ltd., Shenyang, China) was administered twice daily for four consecutive days. Cycloplegic retinoscopy was then performed on the fifth day. In the control group, compound tropicamide 0.5% and phenylephrine 0.5% (SINQI Pharmaceutical Co. Ltd., Shenyang, China) were instilled four times at 5-minute intervals, and retinoscopy was conducted 20 to 25min after the final instillation. All refractions were performed by a single experienced optometrist. BCVA was assessed using a Chinese standard logarithmic visual acuity chart and the results were subsequently converted to the logarithm of the minimum angle of resolution (logMAR) units for analysis. Additionally, axial length (AL) was measured using the Lenstar LS 900 (Haag-Streit AG, Switzerland).

In cases of anisometropic amblyopia, the amblyopic eye was selected for analysis. For isoametropic amblyopia, the eye with worse BCVA was selected; otherwise, the right eye was chosen for analysis if BCVA was equal in both eyes. For each age-matched control case, the right eye of each participant was selected for analysis. If patients were unable to cooperate during measurements involving the right eye or if image quality from the right eye was poor, the left eye was chosen for analysis.

Each participant underwent an SS-OCTA scan (VG200; SVision Imaging Ltd., Luoyang, China). OCTA images were acquired using a raster scan protocol consisting of 512 horizontal B-scans covering a 6 mm×6 mm area centered on the fovea. Each B-scan, containing 512 A-scans, was repeated twice and averaged. Following the examination, image quality was automatically scored by the software on a scale from 1 to 10 (with 10 indicating the highest quality). Scans with a quality score below 7 were either repeated or excluded if the participant was unable to tolerate the procedure.

Choroidal parameters were analyzed using the built-in software, which incorporated AL measurements for image magnification correction. Quantitative analysis was performed within a 3 mm diameter region centered on the fovea to minimize potential confounding from foveal decentration, magnification artifacts associated with hyperopia, and edge effects.

The 3D-CVI was defined as the ratio of choroidal vessel volume (CVV) to total choroidal volume, representing the vascular volume within the Sattler's layer. The software automatically identified this region, generated en face images, segmented choroidal capillaries, and extracted large and medium vessels for analysis. The 3D-CVI was computed automatically.

In this study, concentric circles were used to divide the analyzed region into foveal and parafoveal subregions, as illustrated in Figure 1. The 3D-CVI, three-dimensional CVV (3D-CVV), and CT were then evaluated separately in these two areas, referred to as the foveal and parafoveal 3D-CVI, 3D-CVV, and CT, respectively.

Statistical Analysis All statistical analysis were performed using R software [version 4.3.3 (2024-02-29)]. The Chi-square test was applied to compare gender ratios between the two groups. Normality of continuous variables was assessed using the Shapiro-Wilk test. Variables with a normal distribution are presented as mean±standard deviation, while non-normally distributed variables are reported as median and interquartile range. Paired *t*-tests or Wilcoxon signed-rank tests were used to compare differences between amblyopic and control groups. Generalized estimating equation (GEE) models were employed to adjust for potential confounding effects of age, sex, AL, and spherical equivalent (SE) on CT, 3D-CVI, and 3D-CVV. Univariate and multivariate regression analyses were conducted to evaluate the association between BCVA and foveal as well as parafoveal 3D-CVI. A two-sided *P* value <0.05 was considered statistically significant.

RESULTS

Participant Characteristics The flow of participant inclusion is illustrated in Figure 2. Participants were divided into the amblyopic group and age-matched control group according to the predefined inclusion and exclusion criteria. The demographic and ocular biometric characteristics of the included subjects were presented in Table 1. There were no significant differences in age or gender between the groups, while differences in AL, SE, and BCVA were observed, consistent with the expected distinctions between amblyopic and normal eyes.

Comparison of 3D-CVI and Other Related Choroidal Parameters in Foveal and Parafoveal Regions Between Amblyopic and Normal Group Figure 3A and 3B showed the OCTA output of an amblyopic eye and Figure 3C and 3D showed a normal control eye from two patients. As shown in Table 2, the 3D-CVI in both the foveal and parafoveal regions was lower in amblyopic eyes compared with normal controls. Wilcoxon signed-rank tests showed that these differences were statistically significant (foveal: $P<0.001$; parafoveal: $P<0.001$). After adjusting for age, gender, AL, and SE using GEEs, the differences remained significant (foveal: $P<0.001$; parafoveal: $P=0.003$), indicating that amblyopic eyes exhibited reduced 3D-CVI independent of these confounding factors.

The foveal 3D-CVV in the amblyopic group was 0.1016±0.0229 mm^3, compared to 0.0954±0.0172 mm^3 in the control group ($P=0.2$). Similarly, the parafoveal 3D-CVV was 0.778±0.1522 mm^3 in the amblyopic eyes and 0.733±0.1342 mm^3 in the control eyes ($P=0.2$). After adjusting for age, gender, AL, and SE using GEEs, no statistically significant differences in either foveal or parafoveal 3D-CVV were found between groups (foveal: $P=0.773$; parafoveal: $P=0.869$). These results suggest that, unlike 3D-CVI, 3D-CVV may not exhibit regional differences between amblyopic and normal eyes in this population.

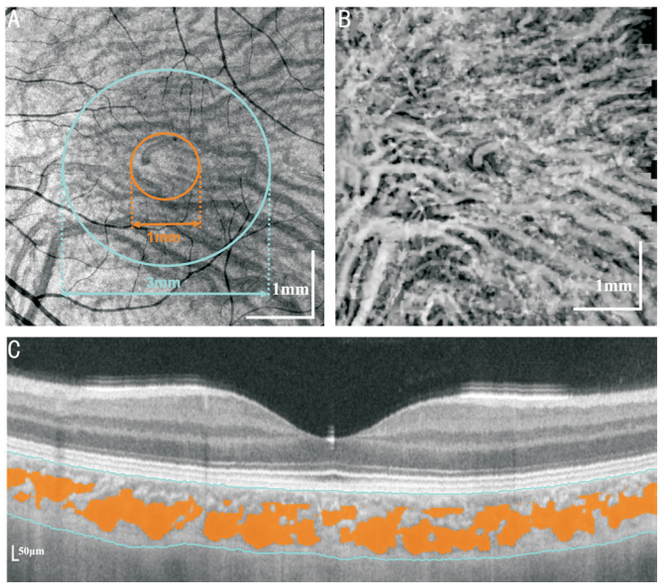

Figure 1 Macular choroidal segmentation and analysis scheme A: Regional partitioning of the macular choroid used for quantitative analysis. Two concentric circles centered on foveal pit were employed to define anatomical subregions. The inner circle (1 mm diameter) delineates the foveal region, and the annular zone between the inner and outer circles (diameter=3 mm) defines the parafoveal region. This segmentation was used for evaluating regional three-dimensional choroidal vascularity index and three-dimensional choroidal vessel volume; B: Schematic representation of the choroidal vascular structure, illustrating the relative distribution of large and medium within the choroid; C: A representative horizontal cross-sectional image passing through the central fovea, showing the analyzed choroidal region and the corresponding structural layers included in the volumetric measurements.

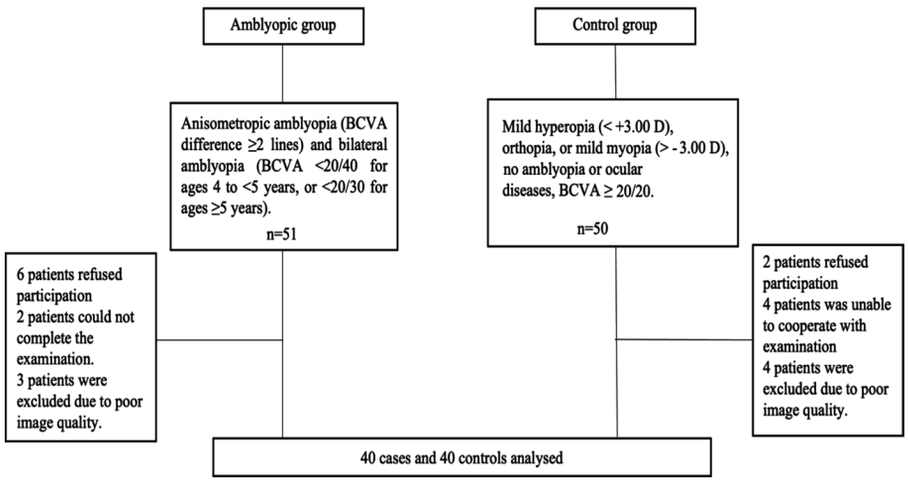

Figure 2 Flowchart of participant inclusion BCVA: Best-corrected visual acuity.

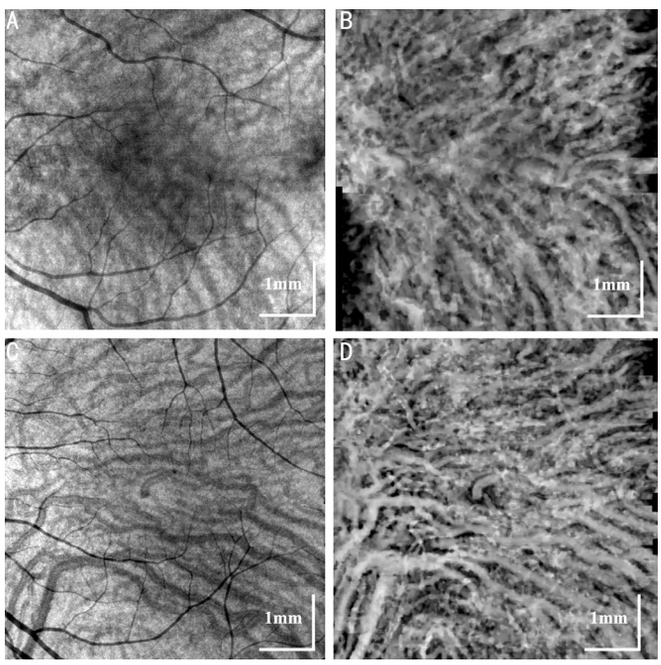

Figure 3 En face retinal and choroidal reconstructions derived from SS-OCTA A: En face retinal optical coherence tomography angiography image acquired from a participant in the amblyopia group, centered on the fovea with a 6 mm×6 mm scan area; B: Corresponding choroidal reconstruction from the same amblyopic eye, demonstrating the segmentation of choroidal vasculature used for volumetric analysis; C: En face retinal optical coherence tomography angiography image from an age-matched participant in the control group, acquired under the same scanning parameters; D: Corresponding choroidal reconstruction from the control eye, illustrating the comparative choroidal vascular structure. SS-OCTA: Swept-source optical coherence tomography angiography.

Table 1 Patient characteristics

Characteristics	Amblyopic group (*n*=40)	Normal group (*n*=40)	*P*
Gender, male/female	21/19	20/20	1.00
Age, y	5.51 (0.945)	5.35 (0.876)	0.471
AL, mm	21.00 (0.933)	22.50 (0.916)	<0.001
SE, D	5.40 (2.73)	0.22 (1.17)	<0.001
BCVA, logMAR	0.43 (0.283)	-0.01 (0.040)	<0.001

AL: Axial length; SE: Spherical equivalent; D: Diopter; BCVA: Best corrected visual acuity; logMAR: The logarithm of the minimum angle of resolution.

The CT was significantly thicker in amblyopic eyes compared to age-matched control eyes in both the foveal and parafoveal regions. Specifically, the mean CT at the foveal region in the amblyopic group was 438±67.3 μm, while that in the control group was 369±74.1 μm (P<0.001). In the parafoveal region, the CT was 419±59.0 μm in the amblyopic group and 353±67.5 μm in the control group (P<0.001). These intergroup differences in CT remained statistically significant after adjusting for age, gender, AL, and SE using GEEs (foveal CT, P=0.0134; parafoveal CT, P=0.0361), suggesting a consistent increase in CT associated with hyperopic amblyopia in preschool children.

Correlation between the BCVA and the 3D-CVI As shown in Table 3, univariate regression analysis revealed a negative correlation between BCVA and 3D-CVI in foveal and parafoveal regions (P<0.001 and P<0.001). After adjusting for age, gender, AL, and SE using multivariate regression analysis, BCVA remained significantly correlated with 3D-CVI in fovea (P=0.024). This model explained 15.7% of the variance in the dependent variable (R^2=0.210; adjusted R^2=0.157; P=0.00316). However, no significant correlation was observed between BCVA and 3D-CVI in parafoveal region (P=0.160).

DISCUSSION

This case-control study found that both foveal and parafoveal 3D-CVI values were significantly lower in hyperopic amblyopic eyes compared to normal control eyes in preschool children aged between 4y and less than 7y. 3D-CVV measurements in amblyopic eyes were comparable to those in normal control eyes, while CT was significantly higher in

Table 2 Comparison of 3D-CVI between the amblyopic group and the normal group

3D-CVI	Median (IQR)		Difference (95%CI)	*P*	
	Amblyopic group	Normal group		Unadjusted[a]	Adjusted[b]
Fovea	0.318 (0.2885-0.3525)	0.381 (0.3460-0.4212)	-0.0696 (-0.1019, -0.0372)	<0.001	<0.001
Parafovea	0.331 (0.2982-0.3589)	0.386 (0.3538-0.4293)	-0.0530 (-0.0874, -0.0185)	<0.001	0.003

[a]Unadjusted value; [b]Adjusted for age, gender, axial length, and spherical equivalent. IQR: Interquartile range; CI: Confidence interval; 3D-CVI: Three-dimensional choroidal vascularity index.

Table 3 Correlation between BCVA and 3D-CVI in fovea and parafovea regions

Items	Univariate regression coefficient			Multivariate regression coefficient		
	B	95%CI	*P*	*β*	95%CI	*P*
Fovea	-0.1019	-0.150, -0.054	<0.001	-0.0808	-0.1508, -0.0109	0.024
Parafovea	-0.0791	-0.125, -0.0336	<0.001	-0.0471	-0.1126, -0.0183	0.160

3D-CVI: Three-dimensional choroidal vascularity index; BCVA: Best corrected visual acuity; CI: Confidence interval.

amblyopic eyes. Furthermore, we first found the lower foveal 3D-CVI values were correlated with poorer BCVA.

The CVI in amblyopic eyes has been investigated in numerous studies; however, the findings remain inconclusive. Most prior research has utilized two-dimensional OCTA image to quantify CVI. Several studies have demonstrated a reduction in CVI in hyperopic amblyopic eyes, consistent with the findings of the present study. For example, Wang *et al*[11] evaluated CVI in preschool-aged children and reported significantly lower values in eyes with hyperopic amblyopia. Similarly, Furundaoturan *et al*[12] observed decreased CVI in school-aged children, and Cevher *et al*[13] extended these findings to the adult population with hyperopic amblyopia.

However, other studies have reported contrasting results. A study conducted in adults reported no significant differences in CVI between amblyopic and fellow eyes[14]. In addition, Baek *et al*[15] and Oren *et al*[16] identified increased CVI in eyes with unilateral anisometropic hyperopic amblyopia, while Kim *et al*[17] also reported elevated CVI values in their study cohort. Notably, Cao *et al*[18] were the first to utilize 3D-CVI analysis to compare amblyopic and normal eyes in anisometropic amblyopia, and similarly found increased 3D-CVI in the amblyopic group.

The heterogeneity observed across studies may arise from several factors. Age influences choroidal structure and vascularity, and prior research has suggested age-related variations in CVI measurements[18-19]. Many previous studies enrolled participants across a relatively broad age spectrum, potentially increasing variability, whereas the present study specifically recruited subjects within a comparatively narrow age range to mitigate this confounding effect. Previous amblyopia treatments, such as optical correction or occlusion therapy, may affect choroidal parameters and thus influence study measurements[17]. It is worth noting that in Cao *et al*'s[18] study, the participants had received prior interventions which may have influenced 3D-CVI measurements and, consequently, the study outcomes. In our study, we enrolled only amblyopic patients without prior therapy, thereby minimizing this potential impact. Methodological variability in CVI estimation—encompassing the use of two-dimensional versus three-dimensional OCTA data, manual versus automated segmentation approaches, and differences in image binarization protocols—may represent an additional source of inconsistency across studies. Although the potential bias between manual and automated segmentation has not been directly quantified, these methodological differences represent a possible source of variability in the results. In the present study, 3D-CVI was calculated using the built-in processing software of the OCTA system, which provides standardized automated segmentation and may improve measurement consistency. AL is also a potential source of confounding, as it can affect the magnification of OCTA images and thus influence measurement results[19]. In the present study, the data were adjusted for AL during analysis, thereby eliminating its impact on OCTA image magnification. In addition, CVI is influenced by refractive status. Previous cross-sectional studies in children[20] have demonstrated that higher hyperopia corresponds to a higher CVI, whereas lower hyperopia is associated with a lower CVI. To ensure that our findings were not confounded by refractive status, we incorporated it into the GEE model and adjusted for its impact on the results.

It remains unclear whether the abnormal choroidal vasculature in amblyopic eyes is causal or secondary to amblyopia. Previous studies have reported that the CVI tends to be reduced in patients with Parkinson's disease, a condition characterized by systemic dopamine deficiency, which may indicate a possible association between dopaminergic activity and choroidal vascular structure[21]. In addition, animal models of amblyopia have shown that monocular form deprivation can lead to regional downregulation of dopamine receptor D1

expression in the dorsal lateral geniculate nucleus, particularly in regions corresponding to the amblyopic eye[22]. While these findings suggest that altered dopaminergic signaling might be involved in the choroidal vascular changes observed in amblyopic eyes, the exact biological mechanisms remain uncertain, and causality cannot be inferred from the current evidence.

Additionally, in contrast to Cao *et al*'s[18] report of higher 3D-CVV in amblyopic eyes, we found no significant difference in 3D-CVV between amblyopic and normal eyes suggesting that hyperopic amblyopia may not cause significant changes in choroidal vessel caliber, but rather exerts its effects predominantly on the stromal compartment.

Moreover, our study revealed that CT in hyperopic amblyopic eyes is thicker than that in normal controls. Even after adjusting for age, gender, SE, and AL using the GEEs method, the CT in amblyopic eyes remained significantly thicker than in the normal control group. This finding contrasts with the results of Cao *et al*[18], who reported similar CT in amblyopic eyes and normal controls. The discrepancies between the two studies may be attributed to differences in the demographics of the included populations, such as age distribution and treatment history. The increased CT observed in amblyopic eyes suggests that amblyopia may impede normal choroidal development. Based on 3D-CVV findings, this effect appears to predominantly involve the stromal component of the choroid.

A further observation from our analysis was that multivariate regression revealed a significant independent negative association between foveal 3D-CVI and BCVA (β=-0.0808, P=0.024), indicating that each unit increase in foveal 3D-CVI corresponded to an improvement of approximately 0.08 logMAR [about 8 letters of Early Treatment Diabetic Retinopathy Study (ETDRS) visual acuity]. Although the adjusted R^2 was relatively low (0.157), suggesting that 3D-CVI accounts for only a modest proportion of BCVA variability, the association remained statistically significant (overall model P=0.00316) after adjusting for key confounding factors, supporting the possibility that choroidal vascular alterations contribute—albeit to a limited extent—to visual function in refractive amblyopia. Nevertheless, the relatively modest R^2 indicates that additional factors may influence BCVA, consistent with previous evidence suggesting that macular retinal vascular indices could also be associated with visual acuity[23]. Currently, there is no evidence confirming an association between 3D-CVI and visual function. Our findings suggest that a reduction in visual acuity may be correlated with a decrease in 3D-CVI. Previous studies have demonstrated delayed structural maturation at the central fovea in amblyopic eyes[24]. As the choroid is the primary source of blood flow and energy supply to the fovea, a decreased CVI may hinder the normal development of the foveal structure, thereby contributing to reduced BCVA. However, due to the cross-sectional nature of this study, a causal relationship cannot be established. Additional well-designed longitudinal investigations are needed to confirm these findings and better understand the temporal relationship between choroidal vascular changes and visual function in amblyopia. Nevertheless, these findings suggest that 3D-CVI may serve as a valuable parameter for monitoring amblyopic changes.

This study has several limitations. First, its cross-sectional design limits the ability to establish causal relationships between hyperopic amblyopia and choroidal vascular changes. Although we discuss a possible role of dopaminergic signaling based on prior human and animal studies, these explanations remain speculative, and longitudinal or mechanistic studies are needed to confirm whether such associations reflect direct biological effects or are mediated by other factors. Second, hyperopia itself has been reported to influence choroidal vascular structure. Ideally, an additional control group of hyperopic children with a comparable degree of hyperopia but normal corrected visual acuity would help isolate 3D-CVI changes attributable solely to amblyopia. However, most children with similar hyperopia exhibit reduced visual acuity, and those who achieve normal acuity after amblyopia treatment are generally older than the target age range of our study population. To address this, we applied the GEE model to adjust for refractive error, AL, age, and sex, and future studies are warranted to further explore the distinct contributions of hyperopia and amblyopia to choroidal vascular changes. Third, the use of two different cycloplegic agents may affect both refractive error and CVI measurements[25-26]. Since 1% atropine can cause prolonged near vision blur, which may significantly impact children's daily activities, we used compounded tropicamide-phenylephrine for cycloplegia in the control group to minimize such effects. Moreover, the use of different cycloplegic agents may introduce slight variations in refractive error measurements. Given the potential influence of different cycloplegic agents on the choroid and the lack of studies comparing their effects, our findings regarding decreased CVI in amblyopic eyes require further validation in future research.

In conclusion, this study demonstrated that both foveal and parafoveal 3D-CVI values were significantly lower in hyperopic amblyopic eyes compared to normal control eyes in preschool children aged between 4y and less than 7y, suggesting that 3D-CVI may serve as a valuable parameter for monitoring structural changes in hyperopic amblyopia, potentially aiding clinicians in early detection of disease progression and in evaluating treatment efficacy during follow-up.

ACKNOWLEDGEMENTS

Authors' Contributions: All authors contributed to the study conception and design. Li YL: Design of the work, drafting the work and revising it critically for important content. Zeng XY, Hua N, and Wang AQ: Acquisition of data. Wang HY: conducted the refractive status evaluation. Qian XH: Conception and design of the work. All authors read and approved the final manuscript.

Data Availability Statement: The data used to support the finding of this study are available from the corresponding author upon request.

Foundations: Supported by the Youth Special Fund of Clinical Research of Tianjin Medical University Eye Hospital (No.2020QN03); Tianjin Key Medical Displine Construction Project (No.TJYXZDXK-3-004A-2).

Conflicts of Interest: Li YL, None; **Hua N,** None; **Zeng XY,** None; **Wang AQ,** None; **Wang HY,** None; **Qian XH,** None.

REFERENCES

1 Cruz OA, Repka MX, Hercinovic A, *et al*. Amblyopia preferred practice pattern. *Ophthalmology* 2023;130(3):P136-P178.

2 von Noorden GK. Histological studies of the visual system in monkeys with experimental amblyopia. *Invest Ophthalmol* 1973;12(10):727-738.

3 Barnes GR, Hess RF, Dumoulin SO, *et al*. The cortical deficit in humans with strabismic amblyopia. *J Physiol* 2001;533(1):281-297.

4 Huang LB, Ding LX, Zheng WD. Microvascular assessment of macula, choroid, and optic disk in children with unilateral amblyopia using OCT angiography. *Int Ophthalmol* 2022;42(12):3923-3931.

5 Huynh SC, Samarawickrama C, Wang XY, *et al*. Macular and nerve fiber layer thickness in amblyopia. *Ophthalmology* 2009;116(9):1604-1609.

6 Lonngi M, Velez FG, Tsui I, *et al*. Spectral-domain optical coherence tomographic angiography in children with amblyopia. *JAMA Ophthalmol* 2017;135(10):1086.

7 Zha Y, Zhuang JF, Feng WQ, *et al*. Evaluation of choroidal thickness in amblyopia using optical coherence tomography. *Eur J Ophthalmol* 2020;30(4):629-634.

8 Aygit ED, Yilmaz I, Ozkaya A, *et al*. Choroidal thickness of children's eyes with anisometropic and strabismic amblyopia. *J AAPOS* 2015;19(3):237-241.

9 Nishi T, Ueda T, Hasegawa T, *et al*. Choroidal thickness in children with hyperopic anisometropic amblyopia. *Br J Ophthalmol* 2014;98(2):228-232.

10 Celik E, Çakır B, Turkoglu EB, *et al*. Evaluation of the retinal ganglion cell and choroidal thickness in young Turkish adults with hyperopic anisometropic amblyopia. *Int Ophthalmol* 2016;36(4):515-520.

11 Wang H, Hu XF, Xin H, *et al*. Assessment of choroidal vascularity and choriocapillaris blood perfusion in Chinese preschool-age anisometropic hyperopic amblyopia children. *Front Pediatr* 2022;10:1056888.

12 Furundaoturan O, Değirmenci C, Akkın C, *et al*. Evaluation of choroidal vascular index in amblyopic patients. *Turk J Ophthalmol* 2022;52(3):168-173.

13 Cevher S, Üçer MB, Şahin T. How does anisometropia affect the choroidal vascularity index *Indian J Ophthalmol* 2022;70(6):2043-2049.

14 Köksaldı S, Kayabaşı M, Kefeli I, *et al*. Choroidal vascular characteristics in anisometropic amblyopia: a comparative analysis. *BMC Ophthalmol* 2025;25(1):301.

15 Baek J, Lee A, Chu M, *et al*. Analysis of choroidal vascularity in children with unilateral hyperopic amblyopia. *Sci Rep* 2019;9:12143.

16 Oren B, Kiziltoprak H, Onder F, *et al*. Evaluation of choroidal vascular structure in hyperopic anisometropic amblyopia. *Beyoglu Eye J* 2023;8(1):32-37.

17 Kim JG, Lee SY, Lee DC. Comparison of retinal and choroidal microvasculature changes in monocular amblyopic and non-amblyopic eyes following short-term patch occlusion treatment. *Curr Eye Res* 2023;48(9):864-872.

18 Cao YW, Zhang YD, Gu XP, *et al*. Choroid vascular changes in hyperopic anisometropia amblyopia using SS-OCTA. *BMC Ophthalmol* 2023;23(1):379.

19 Nishikawa N, Chua J, Kawaguchi Y, *et al*. Macular microvasculature and associated retinal layer thickness in pediatric amblyopia: magnification-corrected analyses. *Invest Ophthalmol Vis Sci* 2021;62(3):39.

20 Qi ZY, Liu XX, Xiong SY, *et al*. Macular and peripapillary Choroidal Vascularity Index in children with different refractive status. *Eye (Lond)* 2024;38(3):606-613.

21 Robbins CB, Thompson AC, Bhullar PK, *et al*. Characterization of retinal microvascular and choroidal structural changes in Parkinson disease. *JAMA Ophthalmol* 2021;139(2):182.

22 Lin DY, Wang ZH, Chen W, *et al*. Regional downregulation of dopamine receptor D1 in bilateral dorsal lateral geniculate nucleus of monocular form-deprived amblyopia models. *Front Neurosci* 2022;16:861529.

23 Wong ES, Zhang XJ, Yuan N, *et al*. Association of optical coherence tomography angiography metrics with detection of impaired macular microvasculature and decreased vision in amblyopic eyes: the Hong Kong children eye study. *JAMA Ophthalmol* 2020;138(8):858.

24 Al-Haddad CE, El Mollayess GM, Mahfoud ZR, *et al*. Macular ultrastructural features in amblyopia using high-definition optical coherence tomography. *Br J Ophthalmol* 2013;97(3):318-322.

25 Xu MY, Li N, Liu Y, *et al*. Effects of tropicamide and compound tropicamide eye drops on ocular biological parameters and choroid thickness in children. *BMC Ophthalmol* 2025;25(1):31.

26 Liu LX, Chen TR, Filipe HP, *et al*. Comparison of cycloplegic effects of atropine and tropicamide in children with refractive error. *Transl Pediatr* 2025;14(7):1616-1623.